CONF-950 [illegible]
SAND95-1383C

CAVITY NUCLEATION AND EVOLUTION IN He-IMPLANTED Si AND GaAs

D. M. FOLLSTAEDT, S. M. MYERS, G. A. PETERSEN and J. C. BARBOUR
Sandia National Laboratories, P. O. Box 5800, Mail Stop 1056, Albuquerque, NM 87185

ABSTRACT

The criteria for forming stable cavities by He^+ implantation and annealing are examined for Si and GaAs. In Si, implanting at room temperature requires a minimum of 1.6 at.% He to form a continuous layer of cavities after annealing at 700°C. The cavities are located at dislocations and planar defects. Implanting peak He concentrations just above this threshold produces narrow layers of cavities at the projected range. In GaAs, room-temperature implantation followed by annealing results in exfoliation of the surface layer. Cavities were formed instead by implanting Ar followed by overlapping He, both at 400°C, with additional annealing at 400°C to outgas the He. This method forms 1.5-3.5 nm cavities that are often on {111} planar defects.

INTRODUCTION

Helium ion implantation has been shown to produce bubbles in Si that outgas during subsequent annealing, leaving empty cavities in the implanted layer [1]. The interior of the cavities is believed to be an ultra-high vacuum, and the clean cavity walls have been used to study surface phenomena, such as H binding on Si [2,3] and Ge [4], trapping of metal impurities from bulk Si [5-7], and the equilibrium shape of cavities [8,9]. To obtain optimum information from such studies, cavity microstructures need to be manipulated, such as varying the internal area or the location of the cavity layer. Since internal cavities are potentially of use for gettering impurities in microelectronic devices, it is important to know the minimum He fluence required for gettering and the nature of lattice defects resulting from implantation and annealing. The width of the cavity layers may become important if the layers are on the front side of wafers near devices. Stable cavities in compound semiconductors such as GaAs are also of interest for studying similar surface-related phenomena.

The following work examines cavities formed in Si by low-fluence He implantation and annealing. A narrow cavity layer forms at the He range for concentrations just above 1.6 at.% He, which is interpreted as the threshold concentration for forming a continuous cavity layer. The cavities form on defects in the Si lattice. Other attempts to vary the structure of cavity layers are discussed. We have also investigated cavity formation in GaAs and found that room temperature implantation followed by annealing produced exfoliation of the surface layer. We therefore developed a method using elevated-temperature implantations of Ar followed by He energies that produced overlapping profiles, with subsequent annealing to outgas the He.

Ion implantation was done into high purity (100) Si or GaAs wafer pieces in a vacuum of $\sim 10^{-6}$ Torr, either at room temperature or at elevated temperatures using a radiatively heated specimen holder. Annealing was done in $\sim 10^{-7}$ Torr vacuum. Cross-section specimens for 200 kV transmission electron microscopy (TEM) were prepared in [110] orientation by gluing two implanted surfaces together and thinning the structure by mechanically polishing (dimpling) and ion-milling perpendicular to the interface. Elastic-recoil detection (ERD) was used to obtain He depth profiles using 24 MeV Si beams entering the specimen at 75° from the surface normal and detecting He forward scattered from the specimen at 30° relative to the incident beam.

MASTER

DISTRIBUTION OF THIS DOCUMENT IS UNLIMITED

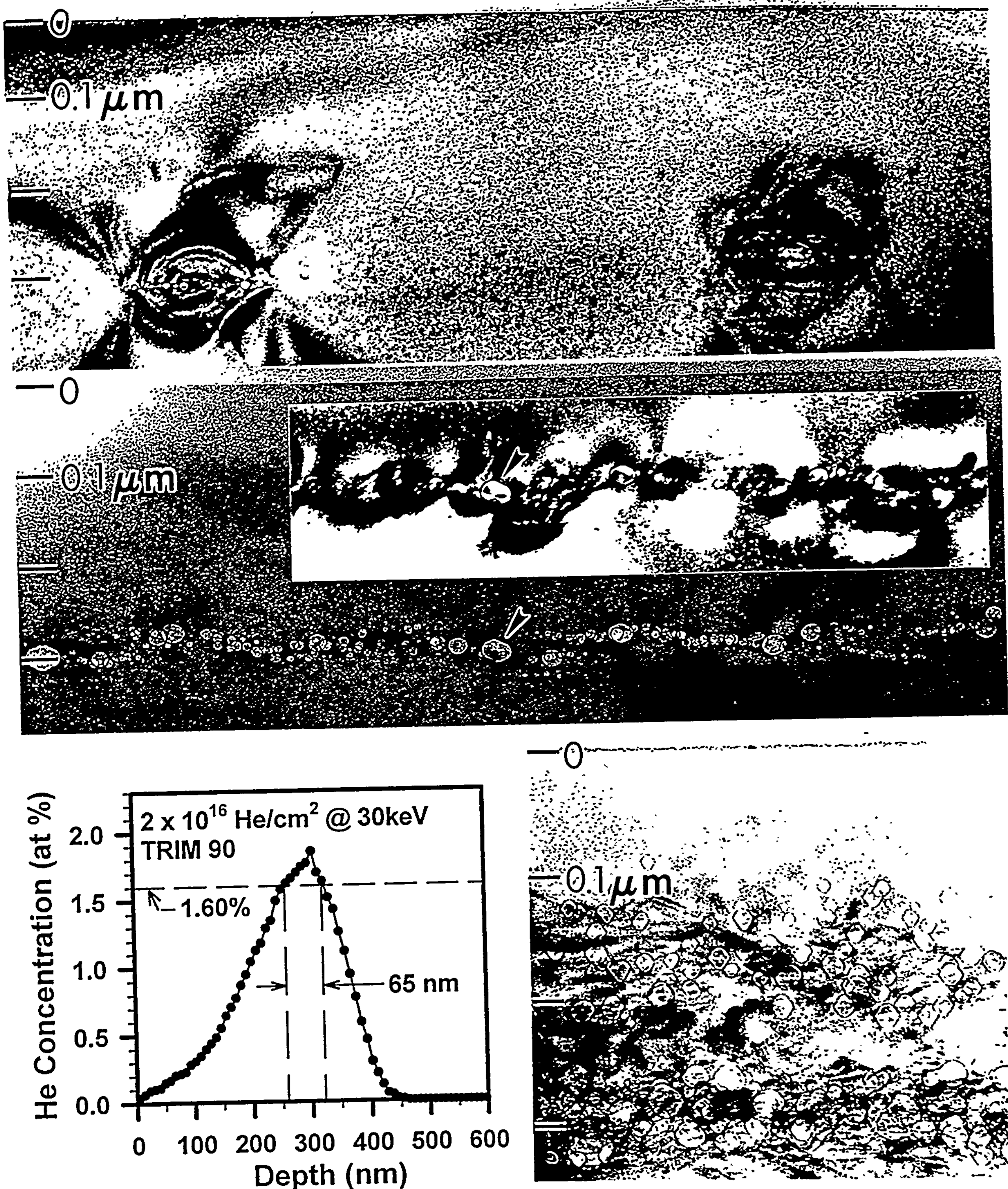

Figure 1. a) [110] cross-section TEM image (-1.3 μm underfocus) of cavity clusters in Si implanted with $1x10^{16}$ He/cm^2 at 30 keV and annealed 1/2 hr. at 700°C. b) Continuous cavity layer (-600 nm underfocus) formed by higher fluence of $2x10^{16}$ He/cm^2. Inset: (111) two-beam image showing strain contrast around lattice defects in the cavity layer. c) Simulated He profile from TRIM90 [11] after scaling to observed $R_p = 300$ nm. Dashed lines indicate the threshold of 1.6 at.% He for forming a continuous cavity layer as inferred from b). d) Cavity structure obtained using the conditions of b) followed by implanting $5x10^{16}$ He/cm^2 at 30 keV and 500°C. Additional cavities are found at a depth of ~180 nm, in front of original layer at $R_p = 300$ nm.

CAVITY FORMATION IN Si

Figure 1a) shows Si implanted with $1x10^{16}$ He/cm^2 at 30 keV after annealing 1/2 hr. at 700°C. The image was obtained by tilting the layer a few degrees off the [110] zone into a kinematic condition without strong diffraction contrast. Fresnel contrast of the cavities was obtained by underfocussing the microscope by 1.3 μm. The cavities are in isolated clusters near the He^+ projected range, R_p = 300 nm. Often there is a larger central cavity (~50 nm across) with smaller cavities (5-10 nm) around it, like one of the clusters in Fig. 1a). The presence of cavities at this fluence agrees with their detection by positrons for a fluence of $8x10^{15}$ He/cm^2 [10]. Residual diffraction contrast around the clusters in Fig. 1a) reflects the presence of strain fields from lattice defects localized on the clusters. Imaging with (111) and (220) two-beam conditions (not shown) indicates the presence of {111} planar defects near the clusters as well as defects parallel to the surface and passing through the cluster centers.

Figure 1b) is from Si implanted with $2x10^{16}$ He/cm^2 at 30 keV after 1/2 hr. at 700°C, and shows a continuous layer of cavities. Some larger cavities (20-40 nm) are seen in the layer; the clusters in Fig. 1a) suggest that the larger cavities may have formed first. Smaller cavities (5-10 nm) lie on continuous curves connecting the larger ones, as if the clusters in Fig. 1a) increased in width until they connected with each other. The continuous curves suggest that the cavities lie along dislocations. The inset in Fig. 1b) was taken with (111) two-beam diffracting conditions and shows strain fields around the entire layer, as expected for connecting dislocations.

The continuous layer is 65 nm wide and located at the range of 30 keV He. Figure 1c) shows a TRIM90 [11] Monte Carlo simulation of the He concentration for $2x10^{16}$ He/cm^2, after scaling the range slightly to fit the observed 300 nm. The He concentration is thought to be the critical parameter in determining whether numerous stable cavities form during the 1/2 hr. anneal at 700°C. The concentration required for a continuous cavity layer lies between the two fluences of Figs. 1a) and 1b), and is close to that of the latter. Using the 65 nm width with the He concentration profile gives a threshold concentration of 1.6 at.% He, as shown by the dashed lines in Fig. 1c). With a fluence of $2x10^{16}$ He/cm^2, the cavity surface area is sufficient to getter $8x10^{14}$ Cu/cm^2, whereas the isolated clusters for $1x10^{16}$ He/cm^2 do not getter significant levels of Cu. Thus $2x10^{16}$ He/cm^2 is also a practical threshold fluence for gettering metal impurities.

We also attempted to increase the cavity area and number density while maintaining a narrow layer by implanting an additional $5x10^{16}$ He/cm^2 into the structure of Fig. 1b). To allow the additional He to collect at the existing layer, the second implantation was done at 500°C. The size and perhaps the density of cavities in the layer at R_p = 300 nm have increased as seen in Fig. 1d). However, a second cavity layer formed at a shallower depth of ~180 nm. Some of the He did not migrate into the first layer but nucleated a new layer instead. The zone with a low density of cavities between the two layers probably reflects the distance over which He could diffuse to existing cavities, which is < 100 nm for this 1/2 hour implantation at 500°C. The TRIM90 simulation for this implantation predicts 2.3 at.% He at the depth of the second layer; thus bubble formation at this depth is consistent with the threshold identified above.

CAVITY FORMATION IN GaAs

Room temperature implantation of $1x10^{17}$ He/cm^2 at 50 keV was found by TEM to produce 1-4 nm bubbles in a damaged layer extending to a depth of 500 nm. Cracks were found at the back of the layer. Since our anticipated uses of the cavities involve annealing and because larger,

gas-free cavities are desirable, specimens implanted with $2x10^{16}$ He/cm^2 to $1x10^{17}$ He/cm^2 were annealed at up to 350°C. All anneals of 250°C and above produced exfoliation of the surface. The Nomarski optical micrograph in Fig. 2 was obtained for $4x10^{16}$ He/cm^2 after annealing 1/2 hr. at 350°C. Some areas show blisters raising the surface while others where the surface layer is absent appear rough. Evolution of the bubbles with temperature and increased pressure apparently broke the overlayer loose, probably at the cracks. Exfoliation was avoided by reducing the fluence to $1x10^{16}$ He/cm^2. We used ERD to monitor the He content remaining in this specimen after 1/2 hr. anneals at increasing temperatures. After annealing at 150°C most of the He remained; at 250°C it dropped to 57%, while at 350°C only 26% of the original He remained. The implanted He becomes mobile at ≥ 250°C; however, at this low fluence much of the He is probably trapped as isolated atoms in the lattice damage rather than being in bubbles.

With the intent of relieving stress in the implanted layer and reducing lattice damage and cracks, a 40 keV implantation of $1x10^{17}$ He/cm^2, was done at 150°C. Analysis with ERD showed that all the He was retained in the implanted layer. Imaging with TEM showed 1-5 nm bubbles in the layer, but cracks were still observed at depths of 300-400 nm. Annealing this specimen at 300°C again resulted in exfoliation of the surface layer. When the implantation temperature for $1x10^{17}$ He/cm^2 was raised to 300°C, ERD indicated that only $7x10^{15}$ He/cm^2 was retained. Neither lattice damage nor cavities were detected with TEM after this implantation. Helium is mobile and leaves the specimen during the 3/4-hour implantation at 300°C without forming bubbles. Mobility at this temperature is consistent with the release noted above.

To provide nucleation sites for bubbles that would retain implanted He, the near-surface layer was pre-implanted with 360 keV Ar^+ to $1x10^{16}$ Ar/cm^2 at 300°C. The GaAs lattice is expected to remain crystalline with this treatment, and the larger Ar atoms should be immobile and stabilize lattice damage. Either Ar sites or related damage might be nucleation centers for He bubbles. When either $5x10^{16}$ He/cm^2 or $1x10^{17}$ He/cm^2 was subsequently implanted at 300°C and 40 keV to overlap the Ar profile, partial exfoliation occurred with only $4x10^{16}$ He/cm^2 retained in the specimen. Lowering the fluence to $3x10^{16}$ He/cm^2 produced no exfoliation and all He was retained. The implanted layer contained 1-4 nm bubbles, often lying on dislocations and planar defects; cracks were also observed. However when the low-fluence specimen was annealed at the higher temperature of 400°C, exfoliation occurred again.

Increasing the implantation temperature to 400°C permitted a higher fluence and He outgassing. Implanting $1x10^{16}$ Ar/cm^2 (360 keV) followed by $5x10^{16}$ He/cm^2 (40 keV) resulted in no exfoliation and retained part of the He, $1.7x10^{16}$ He/cm^2, centered near 300 nm depth, as seen in Fig. 3. Subsequent annealing at 400°C is seen to reduce the content to $4x10^{15}$ He/cm^2 after 5 hr. The cavity microstructure of this annealed specimen is seen in the TEM image in Fig. 4. Cavities appear as small white dots (1.5-3.5 nm in diameter) in this underfocussed image. The cavity layer extends from 0.1 to 0.4 μm with the highest density at a depth of ~0.28 μm, in agreement with the He profile; a few isolated cavities appear beyond this range. The larger cavities often lie along {111} planar defects (one is arrowed), which appear with weak residual diffraction contrast as dark lines. Using characteristic x-rays generated in the microscope, we determined that the implanted Ar is still present in the cavity layer after the 400°C anneal, consistent with our view that Ar is immobile and stabilizes damage. The lattice defects extended to 0.57 μm depth with this treatment. Cracks were not found in the 400°C specimen.

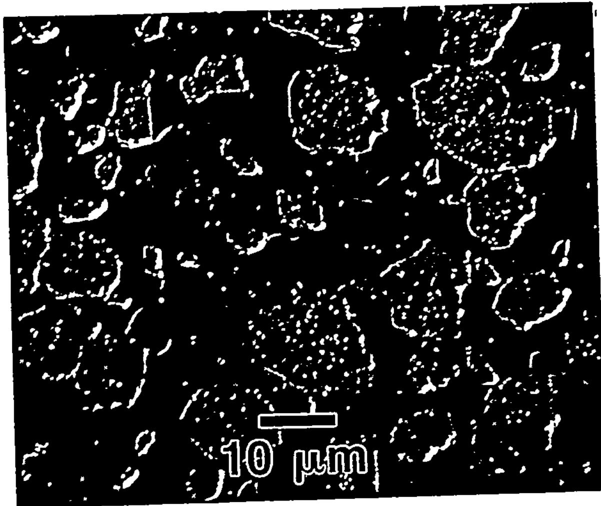

Figure 2. Nomarski optical image of GaAs implanted with $4x10^{16}$ He/cm^2, 40 keV after 1/2 hour at 350°C. Raised blisters are lighted and shadowed as if light were incident from the upper left; exfoliated areas appear rough.

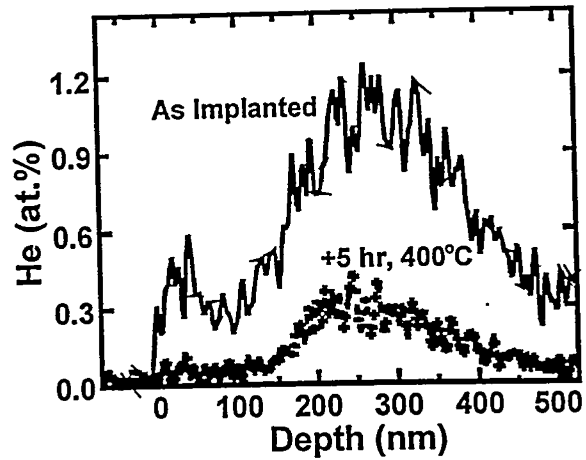

Figure 3. He depth profiles in GaAs implanted with $1x10^{16}$ Ar/cm^2, 360 keV and 400°C, and $5x10^{16}$ He/cm^2, 40 keV and 400°C. Profiles are shown for as-implanted and 5 hr. at 400° annealed conditions.

Figure 4. [110] Cross-section TEM image of cavities in GaAs implanted with $1x10^{16}$ He/cm^2 at 360 keV and 400°C and $5x10^{16}$ He/cm^2 at 40 keV and 400°C, after 5 hr. at 400°C; image obtained at -1.0 μm underfocus. Cavities along a {111} planar defect are indicated by an arrow.

CONCLUSIONS

Cavities are readily formed in Si by room-temperature implantation and annealing. During annealing at 700°C, stable cavities form in association with dislocations and planar defects and the He outgasses. A threshold concentration of 1.6 at.% He was identified for forming a continuous layer of cavities. In GaAs, bubbles form readily by implanting He at up to 150°C,

but the the implanted layer is not stable and does not allow heating to annealing temperatures. It is well known that GaAs is more fragile than Si, and we also find cracks in the He-implanted layer. These features apparently result in exfoliation during annealing.

Isolated, implanted He atoms become mobile at 250°C. Bubbles do not form when He is implanted above this temperature (300 or 400°C), but can be stabilized by pre-implantation of immobile Ar. Lattice damage such as {111} planar defects provide sites for stable bubbles. Thus GaAs is like Si in that thermally stable bubbles are at lattice defects, but for elevated temperatures in GaAs these defects must also be stabilized. Helium outgasses from bubbles in GaAs within several hours at 400°C, similarly to He in bubbles in Si at 700°C. The absence of cracks and stability of the layers indicate that stress is reduced by implanting at 400°C; however this is achieved with the loss of some implanted He. The cavity layers in GaAs appear more damaged than those in Si.

The cavities in GaAs should allow internal surface studies on binding H and other solutes at temperatures up to 400°C. However, they are too small to study crystal facetting. Electrical properties of GaAs are also expected to be altered at cavity layers by the dangling surface bonds.

ACKNOWLEDGMENTS

The authors wish to thank H. J. Stein for contributions during the initiation of studies on He-implanted GaAs. The skillful help of M. P. Moran with cross-section TEM and D. Buller with ERD is much appreciated. This work supported by the Division of Materials Sciences, Office of Basic Energy Sciences of the U. S. Department of Energy under contract DE-AC04-94AL85000.

REFERENCES

1. C. C. Griffioen, J.H. Evans, P.C. de Jong and A. Van Veen, Nucl. Inst. Meth. **B27**, 417 (1987).
2. S. M. Myers, D. M. Follstaedt, H. J. Stein, W. R. Wampler, Phys. Rev. **B47**, 13,380 (1992).
3. W. R. Wampler, S. M. Myers and D. M. Follstaedt, Phys. Rev. **B48**, 4492 (1993).
4. S. M. Myers, H. J. Stein and D. M. Follstaedt, Phys. Rev. **51**, 9742 (1995).
5. V. Rainieri, A. Battaglia and E. Rimini, Nucl. Inst. Meth. **B96**, 249 (1995).
6. J. Wong-Leung, C. E. Ascheron, M. Petravic, R. G. Elliman and J. S. Williams, Appl. Phys. Lett. **66**, 1231 (1995).
7. S. M. Myers, D. M. Follstaedt, D. M. Bishop and J. D. Medernach, in Semiconductor/Silicon 1994, eds. H. R. Huff, W. Bergholz and K. Sumino (The Electrochemical Society, Vol. 94-10, Pennington, NJ, 1994) p. 808.
8. D. M. Follstaedt, Appl. Phys. Lett. **62**, 1116 (1992).
9. D. J. Eaglesham, A. E. White, L. C. Feldman, N. Moriya and D. C. Jacobson, Phys. Rev. Lett. **70**, 1643 (1993).
10. A. van Veen, H. Schut, K. T. Westerduin, M. R. Ijpma, presented at Materials Research Society Fall Meeting, Boston, Nov. 27-Dec 2, 1994; Abstracts, p. 717 (Y9.15).
11. J. F. Ziegler, J. P. Biersack and U. Littmark, The Stopping and Range of Ions in Solids (Pergamon Press, New York, 1985); J. F. Ziegler, private communication, 1990.

DISCLAIMER

This report was prepared as an account of work sponsored by an agency of the United States Government. Neither the United States Government nor any agency thereof, nor any of their employees, makes any warranty, express or implied, or assumes any legal liability or responsibility for the accuracy, completeness, or usefulness of any information, apparatus, product, or process disclosed, or represents that its use would not infringe privately owned rights. Reference herein to any specific commercial product, process, or service by trade name, trademark, manufacturer, or otherwise does not necessarily constitute or imply its endorsement, recommendation, or favoring by the United States Government or any agency thereof. The views and opinions of authors expressed herein do not necessarily state or reflect those of the United States Government or any agency thereof.